

# Two-dimensional spin-imbalanced Fermi gases at non-zero temperature: Phase separation of a non-condensate

Chien-Te Wu, Brandon M. Anderson, Rufus Boyack, and K. Levin  
*James Franck Institute, University of Chicago, Chicago, Illinois 60637, USA*

We study a trapped two-dimensional spin-imbalanced Fermi gas over a range of temperatures. In the moderate temperature regime, associated with current experiments, we find reasonable semi-quantitative agreement with the measured density profiles as functions of varying spin imbalance and interaction strength. Our calculations show that, in contrast to the three-dimensional case, the phase separation which appears as a spin balanced core, can be associated with non-condensed fermion pairs. We present predictions at lower temperatures where a quasi-condensate will first appear, based on the pair momentum distribution and following the protocols of Jochim and collaborators. While these profiles also indicate phase separation, they exhibit distinctive features which may aid in identifying the condensation regime.

Ultracold Fermi gases are a valuable resource for learning about highly correlated superfluids. Their utility comes from their tunability [1] which allows the dimensionality, band structure, interaction strength, and spin imbalance to be freely varied. With these various parameters one can, in principle, simulate a number of important condensed matter systems ranging from preformed pair and related effects in the high  $T_c$  cuprates [2–4] to intrinsic topological superfluids [5–7] and other exotic pairing states.

In this paper we focus on recent experiments [8, 9] of two-dimensional (2D) spin-imbalanced Fermi gases. These address the interesting conflict between the tendency towards enhanced pairing (which is associated with two dimensionality [10]), and spin imbalance which acts to greatly undermine pairing. These imbalance effects are believed [11] to have related effects in studies of color superconductivity and quark-gluon plasmas. In condensed matter systems, lower dimensional imbalanced superfluids are thought to be ideal for observing more exotic phases, such as the elusive LOFF state [12], or algebraic order [13, 14].

The approach we use has been rather successful in addressing 2D low temperature quasi-condensation [15] in balanced gases. In this paper we present predictions for future very low temperature experiments on spin-imbalanced gases. Importantly, our calculations, which find no true long range order, are consistent with the Mermin-Wagner theorem [16]. Following the experiments of Jochim and collaborators [17, 18], we show how quasi-condensation is reflected in the pair-momentum distribution which has a strong peak at low momentum. This peak, which we study throughout the crossover from BCS to BEC, disappears somewhat abruptly at a fixed temperature,  $T_{qc}$ , which denotes quasi-condensation. We find  $T_{qc}$  varies only weakly with the polarization.

A central finding in this paper is that 2D spin-imbalanced systems in a trap exhibit a new form of phase separation involving non-condensed pairs appearing primarily in the center region of the trap. This is to be

contrasted with 3D gases [19, 20] where the phase separation is associated with a true condensate. In the 2D polarized case, because almost all the pairs reside in the central portion of the trap, this leads to a nearly balanced core, as observed in recent experiments [8, 9]. As one goes to larger radii, there are one (at low  $T$ ) or two (at moderate  $T$ ) additional shells. The outermost shell is to be associated with a Fermi gas of majority atoms. An intermediate shell (if it exists) is partially polarized and consists of broken pairs with majority and some minority atoms. Our calculations indicate a necessary but not sufficient condition for quasi-condensation is that a partially polarized intermediate shell will not be present. Instead, there is an abrupt transition from a balanced core to a normal Fermi gas.

There is a sizeable literature on the mutual effects of imbalance and two dimensionality in Fermi superfluids. Experiments have focused on a polaronic interpretation of radio frequency [21] and thermodynamic data. Theory has focused either on the very low temperature region (both the ground state [22, 23] and Kosterlitz Thouless regimes [24, 25]), on possible LOFF phases [26] and on the polaronic limit [27, 28] where the spin imbalance is extreme. Here we consider the entire range of temperatures and polarizations, where there are few theoretical studies [29, 30] using a theory [15] which is consistent with earlier ground state work [22] and with recent experimental studies [17, 18] of 2D balanced gases. We also present a rather successful comparison with experiments [8] performed at moderate temperatures for the in-situ density profiles across the range of BCS to BEC.

*Theoretical formalism.*— The present theory is based on the BCS-Leggett ground state [31] generalized to include polarization effects [32–35] and to higher temperatures. Without showing the details, which have appeared in the recent literature [15], we present two coupled equa-

tions that define a self-consistent fluctuation theory:

$$\sum_{\mathbf{k}} \left[ \frac{1 - f(E_{\mathbf{k}\uparrow}) - f(E_{\mathbf{k}\downarrow})}{2E_{\mathbf{k}}} - \frac{1}{2\epsilon_{\mathbf{k}} + \epsilon_B} \right] = a_0 \mu_{\text{pair}}, \quad (1)$$

$$\sum_{\mathbf{q}} b \left( \frac{\mathbf{q}^2}{2M_B} - \mu_{\text{pair}} \right) = a_0 \Delta^2. \quad (2)$$

Here, the two-band Bogoliubov quasiparticle dispersion  $E_{\mathbf{k}\sigma} = \sigma h + \sqrt{\xi_{\mathbf{k}}^2 + \Delta^2}$  ( $\uparrow, \downarrow$  correspond to  $\sigma = +1, -1$  respectively) is constructed from the bare fermions with excitation spectrum  $\xi_{\mathbf{k}} = \epsilon_{\mathbf{k}} - \mu$  and pairing gap  $\Delta$ . The fermions of mass  $m$  and momentum  $\mathbf{k} = (k_x, k_y)$  have a single particle excitation spectrum  $\epsilon_{\mathbf{k}} = \mathbf{k}^2/2m$ , a fermionic chemical potential  $\mu$ . An effective Zeeman field  $h > 0$  shifts the energy of (majority) spin-up relative to the (minority) spin-down Fermi surfaces. We have also introduced the usual Bose and Fermi distribution functions  $b(x)$  and  $f(x)$ , and included the two-particle binding energy  $\epsilon_B$  [4] to regularize Eq. (1). Throughout this paper we set  $\hbar = 1$ .

The key physics in our system is captured by Eqs. (1)-(2), which reflect the natural equilibrium between fermionic quasiparticles and non-condensed pairs or bosons. Specifically, Eq. (2) introduces non-condensed bosonic degrees of freedom which have momentum  $\mathbf{q}$ , mass  $M_B$ , and chemical potential  $\mu_{\text{pair}}$ . ( $M_B$  and the constant  $a_0$  are calculated from an expansion of a  $t$  matrix describing paired bosons. See the Supplemental Material in Ref. [15] for a precise definition.)

These fluctuations are not present in the strict mean-field theory of BCS; if one sets the pair chemical potential  $\mu_{\text{pair}}$  to zero, then Eq. (1) reduces to the usual mean-field equation for a polarized gas, specifying the gap parameter  $\Delta$ . Including these fluctuations then allows one to solve for the two unknowns:  $\Delta$  and  $\mu_{\text{pair}}$ . The fermions are associated with the energy  $\Delta$  needed to break apart pairs, and the non-condensed bosonic pairs have a self-consistently determined chemical potential  $\mu_{\text{pair}}$ , which depends on the pairing gap  $\Delta$ . Here the number density of pairs (bosonic number) is given by  $n_B = a_0 \Delta^2$ . The more non-condensed bosons which are present, the larger the pairing gap. That these bosonic degrees of freedom cannot condense in 2D allows us to incorporate the constraints of the Mermin-Wagner theorem. We can think of these as the introduction of fluctuation effects.

In experiments, the effective Zeeman field  $h$  and total chemical potential  $\mu$  derive from a magnetization  $m = n_{\uparrow} - n_{\downarrow}$  and number density  $n = n_{\uparrow} + n_{\downarrow}$ . Thus we set the fermionic chemical potentials using the number equation

$$n_{\sigma} = \frac{1}{2} \sum_{\mathbf{k}} \left[ \left( 1 - \frac{\xi_{\mathbf{k}}}{E_{\mathbf{k}\sigma}} \right) f(-E_{\mathbf{k}\sigma}) + \left( 1 + \frac{\xi_{\mathbf{k}}}{E_{\mathbf{k}\sigma}} \right) f(E_{\mathbf{k}\sigma}) \right] \quad (3)$$

for the number density of species  $\sigma = -\bar{\sigma}$ .

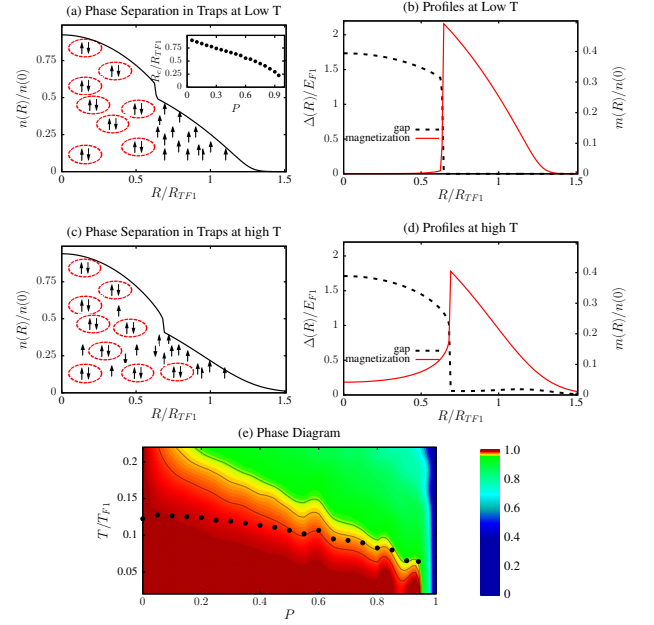


FIG. 1. This figure contrasts the nature of phase separation in a harmonic trap at low temperatures ((a) and (b)) where quasi-condensation occurs ( $T/T_{F1} = 0.06$ ) and moderate temperatures ((c) and (d)) ( $T/T_{F1} = 0.22$ ) more appropriate to experiments [8, 9]; the binding energy is fixed at  $E_{F1}/\epsilon_B = 0.75$ . Black lines represent the local density  $n(R)$  in (a) and (c), while in (b) and (d) the pairing gap  $\Delta(R)$  is black (dashed) and the magnetization  $m(R)$  is red. Panel (a) shows the “two shell” structure: the core region, next to a fully polarized region, is occupied only by pairs. The radius at which the gap turns off abruptly at low  $T$  is indicated as an inset in (a). The density profile in panel (c) exhibits a “three shell” structure: the almost balanced core region is followed by a transition region that is partially polarized and the edge is fully polarized. Finally panel (e) presents a phase diagram where the color contours indicate the central balance ratio,  $\tilde{p}(0) = n_{\downarrow}(0)/n_{\uparrow}(0)$ , of minority to majority atoms at the trap center. The three contours mark values of 99%, 98%, and 97% for this ratio. The black dots mark the onset of quasi-condensation, as defined in Eq. (4).

To account for the trapping potential, we apply the local density approximation (LDA) to a system with total atom number  $N_{\uparrow}$  ( $N_{\downarrow}$ ) of majority (minority) carrier. Here we replace  $\mu \rightarrow \mu(R) \equiv \mu_0 - \frac{1}{2}m\omega^2 R^2$ , and  $\Delta \rightarrow \Delta(R)$ , where  $\mu_0$ ,  $\omega$ , and  $R$  represent the central fermionic chemical potential, the trap frequency, and position respectively. Derived quantities such as the magnetization  $m(R)$ , number density  $n(R)$ , and pair mass  $M_B(R)$  gain local dependence. However, the effective Zeeman field is homogeneous throughout the trap. Where relevant, we express energy and local position in units of the majority spin Fermi energy,  $E_{F1} = \omega \sqrt{2N_{\uparrow}}$ , and Thomas-Fermi radius  $R_{TF1} = \sqrt{2E_{F1}/m\omega^2}$  respectively; we take  $\omega/E_{F1} = 1/40$  comparable to Ref. [8].

In what follows, it will be convenient to define a local polarization  $p(R) = m(R)/n(R)$ , a total polariza-

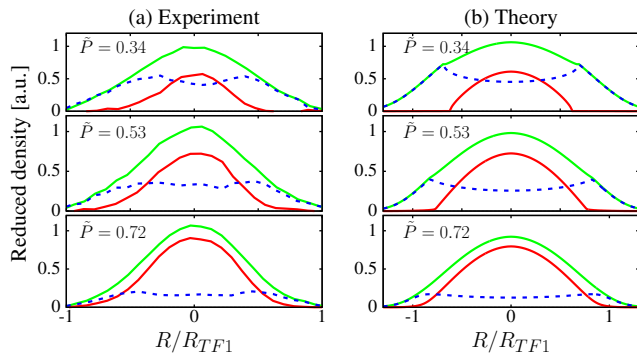


FIG. 2. Comparison of integrated column density profiles of (a) experiment [8] and (b) theory for a trapped system with  $E_{F1}/\epsilon_B = 0.75$  and  $T/T_{F1} = 0.22$ . The green, red, and blue curves are the reduced densities (see [8] for definition) of the majority, minority, and magnetization (difference), respectively. The legend indicates the total balance ratio  $\tilde{P} = N_{\downarrow}/N_{\uparrow}$ . A transition to a nearly balanced core is seen in both theory and experiment.

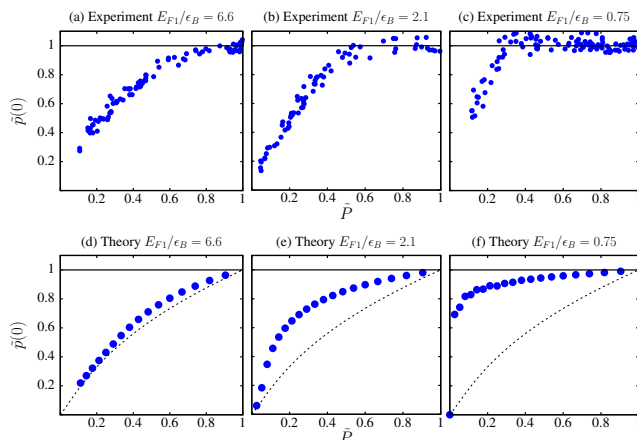


FIG. 3. Comparison of theoretical and experimentally measured [8] values of the central balance ratio  $\tilde{p}(0) = n_{\downarrow}(0)/n_{\uparrow}(0)$ , at  $T/T_{F1} = 0.22$ . The dashed curves give the ideal Fermi gas limit ( $\epsilon_B = 0$ ); the solid black curves are guides to the eye.

tion  $P = (N_{\uparrow} - N_{\downarrow}) / (N_{\uparrow} + N_{\downarrow})$ . To connect with recent experiments [8], we will also define a “balance ratio”  $\tilde{p}(R) = n_{\downarrow}(R)/n_{\uparrow}(R)$ , and similarly for a total balance ratio  $\tilde{P} = N_{\downarrow}/N_{\uparrow}$ .

*Numerical results.*— Figure 1 serves to clarify the concept of phase separation in a trapped 2D gas for both low ( $T/T_{F1} = 0.06$ ) and moderate temperatures ( $T/T_{F1} = 0.22$ ) regimes. The former are applicable to the quasi-condensation regime discussed below, while the latter are closer to the regimes studied experimentally [8, 9]. We consider an intermediate binding energy  $E_{F1}/\epsilon_B = 0.75$ . The density profiles as a function of position in these two temperature regimes are plotted in panels (a) and (c), along with a cartoon illustration of the nature of the gas, as the radius changes. Panels (b) and

(d) provide useful information on the gap profiles (black dashed) and magnetization profiles (red). The radius at which the gap turns off abruptly at low  $T$  is indicated as an inset in (a).

At the lower temperatures there is an abrupt boundary separating a fully paired state in the core (indicated by the paired spins in the cartoon) and a non interacting fully polarized gas of majority spins (also represented in a cartoon fashion). We refer to these profiles as containing only “two shells”: composite bosons at the core and majority fermions surrounding it. Importantly, one sees that the magnetization in Fig. 1(b) and the gap both change nearly discontinuously.

Although the number density profile in Fig. 1(c) behaves similarly to its low- $T$  counterpart, one sees here (using information about the calculated gap, local polarization, and magnetization), that there are now “three shells” in the structure, as shown in the cartoon. The core region contains mostly non-condensed pairs with very little magnetization. As one goes away from the trap center, the local magnetization initially increases resulting in a central shell. Finally, toward the edge of the trap where the magnetization drops, the gas is non-interacting ( $\Delta(R) = 0$ ) and fully polarized.

These calculations suggest that the magnetization versus position  $R$  serves as a kind of thermometry. In particular, that we are able to associate the lower- $T$  behavior with the existence of a (quasi-)condensate, can be inferred from the phase diagram plotted in Fig. 1(e). Here the vertical and horizontal axes represent temperature  $T$ , and total polarization  $P$ , respectively. As indicated in the legend, the colors more precisely correspond to the ratio of minority to majority spins at the trap center. The three contours mark 99%, 98%, and 97% for the ratio. The black dots on the phase diagram show where we find pair (quasi-)condensation, as will be discussed below. It should be clear that this quasi-condensate essentially always appears in conjunction with our “two shell” profiles.

*Comparison with Experiment.*— The general picture described above has consequences that can be directly compared to recent experiments. In Fig. 2, as in experiment [8], we plot “column density” profiles for majority and minority components in the trap along with the difference profile (local magnetization), for three different values of the balance ratio  $\tilde{P}$ . (The total polarization increases as one goes upward on the three panels). The counterpart experimental data is plotted on the left along with theory curves on the right. In the calculations, we consider fixed moderate temperature  $T/T_{F1} = 0.22$ .

This observation of phase separation of a non-condensate underlines some of the same points as in the 2D density profiles shown in Fig. 1. Here, however, one sees how this physics is reflected in actual experiments. Indeed, there is a particularly interesting indicator of this form of phase separation. The ratios of minority to ma-

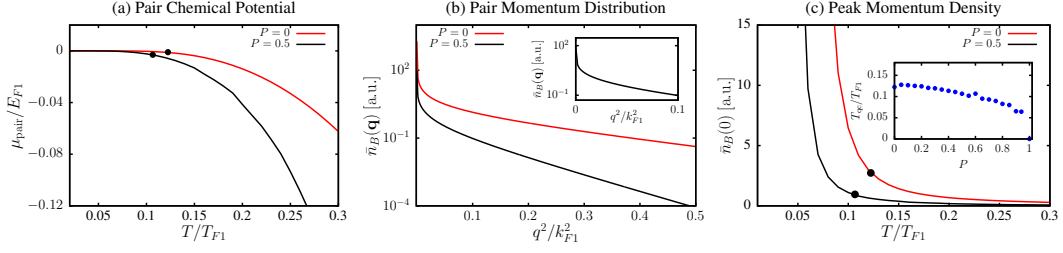


FIG. 4. Characteristics of quasi-condensation at a binding energy  $E_{F1}/\epsilon_B = 0.75$ . Pair chemical potential (a) for a polarized (black,  $P = 0.5$ ) and unpolarized (red) Fermi gas. The small and non-zero size of  $\mu_{\text{pair}}$  reflects an exponential suppression at low temperatures [15]. (b) This leads to a low-momentum peak in the pair momentum distribution  $n_B(\mathbf{q} = 0)$  at low temperatures. (c) The dependence of the  $n_B(0)$  peak on temperature allows the extraction (dots) of  $T_{\text{qc}}$  in Eq. (4).

majority 2D densities at the trap center have been measured by Thomas and collaborators [8]. These experiments investigate the variation as one crosses from more BCS to more BEC like behavior. They observe (see Fig. 3, top panels) the somewhat striking result that, away from the BCS regime, there is a rather abrupt transition from a balanced core to an unpaired phase at a critical polarization (which is presumably temperature dependent). The constancy of the data points indicates the very strong tendency to maintain maximal pairing until it is no longer possible. The abrupt drop occurs presumably because one has crossed the so-called  $T^*(P)$  line. This temperature  $T^*$  marks the end-point of a pairing gap, often called the pseudogap.

In Fig. 3 we present a comparison between theoretical and experimental results, plotting the central balance ratio  $\tilde{p}(0)$  as a function of the total balance ratio  $\tilde{P}$ . In our theoretical analysis we fix the temperature for all panels at  $T/T_{F1} = 0.22$ . In the stronger pairing cases (with  $E_{F1}/\epsilon_B = 0.75$  and  $E_{F1}/\epsilon_B = 2.1$ , as shown in the two panels to the right) the persistence of a balanced core for a range of total polarizations is observed. The theory curves are not quite as flat as in experiment, which suggests that theory temperatures are slightly high in comparison; in both cases the downward departure is reasonably sudden.

These curves reflect simple changes in the trap profile; as  $\tilde{P}$  increases, the boundary between balanced and imbalanced regions moves toward the trap center, (shown in the inset to Fig. 1(a)) while not affecting the magnetization at the precise “center”. For smaller  $\epsilon_B$  at finite  $T$ , the balanced core is narrower and the magnetization at the center also increases more rapidly as compared to larger  $\epsilon_B$ . At sufficiently high  $P$ , for this temperature regime the system is driven normal and the profiles are those of an ideal Fermi gas.

*Quasi-condensation at very low temperatures.*— We turn now to the lowest temperature regime away from  $T \equiv 0$ , where true long-range order is not possible, at least for a homogeneous system in the thermodynamic limit. The evidence from experiments [17, 18] on 2D spin-balanced Fermi gases suggests that the bosonic degrees

of freedom (accessed by rapid magnetic field sweeps) exhibit strong  $|\mathbf{q}| \rightarrow 0$  peaks in their momentum distribution, represented by a trap-average, denoted  $\bar{n}_B(\mathbf{q})$ , of  $n_B(\mathbf{q}) = b(\mathbf{q}^2/2M_B - \mu_{\text{pair}})$  appearing in Eq. (2). What is most significant [15] is that these peaks disappear rather abruptly at a particular temperature,  $T_{\text{qc}}$ , which one associates with the onset of quasi-condensation.

Following the same analysis for a spin-imbalanced Fermi gas, in Fig. 4(a) we plot the pair chemical potential  $\mu_{\text{pair}}$  at the trap center for an unpolarized (in red) and a polarized gas (in black,  $P = 0.5$ ). We find  $\mu_{\text{pair}}$  serves to determine the size of the peak structure in  $\bar{n}_B(\mathbf{q})$  as can be seen from Eq. (2). In both the balanced and imbalanced cases, this pair chemical potential is found to nearly vanish at low temperatures, signifying a bosonic momentum distribution that is sharply peaked but never acquires a macroscopic condensate. Moreover, it is seen that the effects of spin imbalance are relatively minor, resulting in only a small quantitative shift in  $\mu_{\text{pair}}$  compared to the balanced case.

Figure 4(b) presents the counterpart plots of  $\bar{n}_B(\mathbf{q})$  versus  $\mathbf{q}$  where the two curves correspond to  $P = 0$  in red and  $P = 0.5$  in black. The latter is enlarged in the inset, where the peak in the momentum distribution at  $\mathbf{q} = 0$  is evident. The temperature dependence of this peak is reflected in Fig. 4(c). The solid dots indicate the temperature,  $T_{\text{qc}}$ , at which the pair chemical potential begins to deviate from effectively zero. Taking the deviation point as in Ref. 15 (which roughly corresponds to about a 1% shift from the background) yields

$$k_B T_{\text{qc}} \approx \frac{\pi}{2.3} \frac{\hbar^2 n_B(T = T_{\text{qc}})}{M_B(T = T_{\text{qc}})}, \quad (4)$$

where we use the Bose number density  $n_B(T = T_{\text{qc}})$  and the pair mass  $M_B(T = T_{\text{qc}})$  at the trap center. The inset of Fig. 4(c) presents a plot of this quasi-condensation temperature as a function of total polarization. The effects of polarization on this temperature are relatively weak, presumably because of the phase separated and fully balanced spin core.

These same results are summarized by the black dots in Fig. 1(e) which presents a generalized phase diagram



indicating the  $P$ ,  $T$  parameters at which there is phase separation, as represented by the imbalance at the trap center. We note that the characteristic inner-core radius, which is plotted as an inset in Fig. 1(a), shows that for moderate polarizations the range in radii over which one has pairing (and therefore quasi-condensation) is restricted. This makes it difficult to perform the analysis that addresses power laws vs exponential fitting functions in the Fourier transform of  $\bar{n}_B(\mathbf{q})$ , which was identified [18] with  $g_1(r)$ . For the unpolarized case, such an analysis [15] further substantiated the identification of  $T_{qc}$  with the expression in Eq. (4).

*Conclusions.*— A goal of this paper has been to emphasize the distinction between the paired (normal state) and the lower temperature quasi-condensed phase of a 2D polarized gas. We show that both are associated with a balanced or nearly balanced core, but the nature of the related phase separation is somewhat distinctive, leading to more abrupt boundaries when quasi-condensation is present. Proving the existence or non-existence of true phase coherence would lead to a significant advance in the understanding of the physics of 2D Fermi gases. As in previous work [15, 17, 18] true superfluidity in 2D has not been established here or in experiments. This will require future experimental probes related to coherence features, including interference measurements, or detection of the presence of collective modes in Bragg scattering.

*Note Added.*— Near completion of the manuscript we learned of a recent preprint [9] which addressed experimentally many of the same findings as contained in our manuscript.

*Acknowledgments.*— This work was supported by NSF-DMR-MRSEC 1420709. We thank J. Thomas for stimulating conversations and for sharing his data. We are grateful to W. Bakr and D. Mitra for useful discussions and information about their experiment.

---

[1] W. Ketterle and M. W. Zwierlein, in *Ultra-cold Fermi Gases*, edited by M. Inguscio, W. Ketterle, and C. Salomon (Italian physical society, 2007) p. 95.  
[2] Q. J. Chen, J. Stajic, S. N. Tan, and K. Levin, *Phys. Rep.* **412**, 1 (2005).  
[3] A. Perali, P. Pieri, G. C. Strinati, and C. Castellani, *Phys. Rev. B* **66**, 024510 (2002).  
[4] V. M. Loktev, R. M. Quick, and S. G. Sharapov, *Physics Reports* **349**, 1 (2001).  
[5] H. Zhai, *Rep. Prog. Phys.* **78**, 026001 (2015).  
[6] C. Zhang, S. Tewari, R. Lutchyn, and S. DasSarma, *Phys. Rev. Lett.* **101**, 160401 (2008).

[7] M. Iskin and A. L. Subaşı, *Phys. Rev. Lett.* **107**, 050402 (2011).  
[8] W. Ong, C. Cheng, I. Arakelyan, and J. E. Thomas, *Phys. Rev. Lett.* **114**, 110403 (2015).  
[9] D. Mitra, P. Brown, P. Schauss, S. Kondov, and W. Bakr, “Phase separation and pair condensation in a spin-imbalanced 2d fermi gas,” (2016), arXiv/1604.01479.  
[10] M. Randeria, J.-M. Duan, and L.-Y. Shieh, *Phys. Rev. B* **41**, 327 (1990).  
[11] E. Gubankova, A. Schmitt, and F. Wilczek, *Phys. Rev. B* **74**, 064505 (2006).  
[12] R. Casalbuoni and G. Nardulli, *Rev. Mod. Phys.* **76**, 263 (2004).  
[13] J. M. Kosterlitz and D. J. Thouless, *J. Phys. C: Solid State* **6**, 1181 (1973).  
[14] V. Berezinskii, *Sov. Phys. JETP* **34**, 610 (1972).  
[15] C.-T. Wu, B. M. Anderson, R. Boyack, and K. Levin, *Phys. Rev. Lett.* **115**, 240401 (2015).  
[16] N. D. Mermin and H. Wagner, *Phys. Rev. Lett.* **17**, 1133 (1966).  
[17] M. G. Ries, A. N. Wenz, G. Zürn, L. Bayha, I. Boettcher, D. Kedar, P. A. Murthy, M. Neidig, T. Lompe, and S. Jochim, *Phys. Rev. Lett.* **114**, 230401 (2015).  
[18] P. a. Murthy, I. Boettcher, L. Bayha, M. Holzmann, D. Kedar, M. Neidig, M. G. Ries, a. N. Wenz, G. Zürn, and S. Jochim, *Phys. Rev. Lett.* **115**, 10401 (2015).  
[19] G. B. Partridge, W. Li, R. I. Kamar, Y. A. Liao, and R. G. Hulet, *Science* **311**, 503 (2006).  
[20] Y. Shin, M. W. Zwierlein, C. H. Schunck, A. Schirotzke, and W. Ketterle, *Phys. Rev. Lett.* **97**, 030401 (2006).  
[21] Y. Zhang, W. Ong, I. Arakelyan, and J. E. Thomas, *Phys. Rev. Lett.* **108**, 235302 (2012).  
[22] .  
[23] G. J. Conduit, P. H. Conlon, and B. D. Simons, *Phys. Rev. A* **77**, 053617 (2008).  
[24] J. Tempere, S. N. Klimin, and J. T. Devreese, *Phys. Rev. A* **79**, 053637 (2009).  
[25] S. N. Klimin, J. Tempere, J. T. Devreese, and B. Van Schaeybroeck, *Phys. Rev. A* **83**, 063636 (2011).  
[26] D. E. Sheehy, *Phys. Rev. A* **92**, 053631 (2015).  
[27] M. M. Parish, *Phys. Rev. A* **83**, 051603 (2011).  
[28] M. M. Parish and J. Levinsen, *Phys. Rev. A* **87**, 033616 (2013).  
[29] M. J. Wolak, B. Grémaud, R. T. Scalettar, and G. G. Batrouni, *Phys. Rev. A* **86**, 023630 (2012).  
[30] M. A. Resende, A. L. Mota, R. L. S. Farias, and H. Caldas, *Phys. Rev. A* **86**, 033603 (2012).  
[31] A. J. Leggett, in *Modern Trends in the Theory of Condensed Matter* (Springer-Verlag, Berlin, 1980) pp. 13–27.  
[32] Y. He, C.-C. Chien, Q. Chen, and K. Levin, *Phys. Rev. B* **76**, 224516 (2007).  
[33] C.-C. Chien, Q. J. Chen, Y. He, and K. Levin, *Phys. Rev. A* **74**, 021602(R) (2006).  
[34] C.-C. Chien, Q. J. Chen, Y. He, and K. Levin, *Phys. Rev. Lett.* **97**, 090402 (2006).  
[35] Q. Chen, Y. He, C.-C. Chien, and K. Levin, *Phys. Rev. B* **75**, 014521 (2007).